Available online at www.sciencedirect.com
SCIENCE DIRECT®

ELSEVIER

Polymer 46 (2005) 6025–6034

polymer

www.elsevier.com/locate/polymer

Preparation and characterization of titanate-modified Boehmite–polyamide-6 nanocomposites

Ceren Özdilek[a], Krzysztof Kazimierczak[b], Stephen J. Picken[a,*]

[a]*Department of Polymer Materials and Engineering, Delft University of Technology, Julianalaan 136, 2826 BL Delft, The Netherlands*
[b]*University of Technology in Wroclaw, 50-373 Wroclaw, Poland*

Received 7 February 2005; received in revised form 11 May 2005; accepted 16 May 2005
Available online 15 June 2005

Abstract

This work reports the use of titanate-modified Boehmite particles in making polyamide-6 nanocomposites complementary to our previous work, which discussed the use of unmodified Boehmite. A new method for the surface modification of Boehmite has been applied. The characterization methods include transmission electron microscopy (TEM), atomic absorption spectroscopy (AAS), thermogravimetric analysis (TGA), differential scanning calorimetry (DSC) and dynamical mechanical analysis (DMA). DSC reveals that addition of titanate-modified Boehmite favours the formation of the γ-phase, especially at higher concentrations. Melting temperatures of α- and γ-phases show a slight decrease with Boehmite concentration. The samples have almost identical degree of crystallinity. Upon addition of the titanate-modified Boehmite particles, a two-fold increase in the storage modulus of the matrix polymer is obtained. The advantage of using titanate-modified Boehmite is that higher amounts of nano-particles can be introduced into the matrix polymer, and therefore higher modulus values can be obtained.

Keywords: Boehmite; Surface modification; Nanocomposites

1. Introduction

Surface modification of colloidal particles has been an important area of interest in physical chemistry during the last couple of years. The demand for surface modification of colloids originates for various reasons. When colloidal particles are surface-modified, they can be examined in a wide variety of solvents or in mixtures with organic species or polymers, which can be interesting from an academic point of view. On the other hand, being able to mix colloids with different polymer systems can stimulate the development of new hybrid materials, which is important in nanocomposite applications. In this introduction, we will first briefly discuss various surface modification methods and then proceed to describe several routes that were considered for making Boehmite–polymer nanocomposites.

Boehmite, also known as γ-AlOOH, is the starting material in the production of γ- and α-Al_2O_3 [1]. These aluminium oxides have important application areas such as technical ceramics, thin solid films and catalysis [2]. Since the properties of aluminium oxides are very much dependent on the properties of Boehmite as the starting material, preparation of Boehmite particles with well-defined size and shape becomes an important issue. In addition to its application areas, synthetic Boehmite is important for the academic interest and it has been extensively studied as a well-defined model system to investigate the colloidal nematic phase [3–6]. Boehmite particles used in our study have sizes on the nanometre scale and they have a rod-like shape with a high extent of anisotropy. After the synthesis, they are obtained as stable aqueous dispersions, which are thixotropic and birefringent. Due to their high anisotropy, they are capable of forming nematic phase after a certain critical concentration.

1.1. Surface modification methods

The surface modification of colloidal particles is a challenging issue. The stability of colloids depends on the delicate balance between inter-particle forces, which are

---

* Corresponding author. Tel.: +31 15 2786946; fax: +31 15 2787415.
E-mail address: s.j.picken@tnw.tudelft.nl (S.J. Picken).

0032-3861/$ - see front matter © 2005 Elsevier Ltd. All rights reserved.
doi:10.1016/j.polymer.2005.05.065

mainly electrical double-layer repulsion and Van der Waals attraction [3]. Provided that electrical double-layer repulsions in the system are not sufficiently strong, attraction prevails and agglomeration of the particles occurs. As the inter-particle forces strongly depend on the surface charges and pH/ionic strength of the medium, these parameters should be controlled during the surface treatment procedure.

Many different surface modification methods exist in literature [4–6]. One of the most common methods is the use of surfactants. Surfactant molecules that are oppositely charged with respect to the surface attach to the particles by means of ionic attractions. Colloidal stability is obtained by covering the surface with surfactant molecules, which, due to their long alkyl parts, provide a steric barrier against agglomeration of the particles. The main disadvantage is the lack of covalent bonds between the surfactant molecule and the colloidal species, which makes the system less stable against changes in the chemical environment or application of high shear forces, ultrasonication, etc.

A better alternative is the use of coupling agents. Coupling agents can covalently bond to the surface to be modified and act as compatibiliser between two dissimilar systems, such as organic polymers and inorganic surfaces. According to Levering, three main types of coupling agents can be distinguished: zirconates/titanates, silanes and zircoaluminates [7]. Among these, silanes form the most widely studied group. Since their first successful use reported in the 1940s, they have been widely used in many compositions. The silane coupling-agents are claimed to be capable of bonding a vast number of inorganic fillers to many polymeric matrices. The general structure can be described as follows [8]:

$$\mathbf{(RO\text{-})_3\text{-}Si\text{-}(\text{-}R'Y)}$$

where R is the hydrolysable group; and R′Y is the organofunctional group. The advantages of silane compounds are: water solubility (or insolubility, depending on the organofunctional part) and the presence of a highly stable Si–C bond, which is not hydrolysable.

Zircoaluminates form a relatively new class of coupling agents. Their general structure is particularly complex. They exhibit excellent adhesion to inorganic surfaces, which is due to the large inorganic moiety in the structure. In the literature, the use of zircoaluminates to modify aluminium oxide particles has already been reported, which yielded an improved dispersion of the particles in a polypropylene matrix [9].

As for the titanate coupling agents, the general structure is as follows

$$\overset{(1)}{(\mathrm{RO}\,\text{-})_n}\text{-}\overset{(2)}{\mathrm{Ti}}\text{-}(\text{-}\,\overset{(3)}{\mathrm{O}}\,\overset{(4)}{\mathrm{X}}\,\overset{(5)}{\mathrm{R'}}\,\overset{(6)}{\mathrm{Y}}\,)_{4-n}$$

These agents seem to have a large number of superior features over the other coupling agents. In the molecule, six main functional sites can be distinguished (1) hydrolysable group reactive towards surface hydroxyl or protons; (2) tetravalent titanium atom, which forms a Ti–O bond capable of dissociation and subsequent reaction; (3) X: binder functional group such as phosphato, pyrophosphato, sulfonyl, carboxyl, for properties like burn rate control, anticorrosion, etc.; (4) R′: thermoplastic functional group such as isopropyl, butyl, octyl, aromatic benzyl etc.; (5) Y: thermosetfunctional group such as methacryl, mercapto, amino, etc.; (6) 4-n: organofunctionality (mono-, di- or tri-). Monte et al. have studied these titanate coupling agents in detail and have provided a major contribution to the field [10].

1.2. Methods for preparation of Boehmite nanocomposites

So far in our research on Boehmite–polymer nanocomposites, several attempts were made in order to find a good modification method for the Boehmite particles. Boehmite particles were perfectly stable in their aqueous dispersions, but in order to stabilise them in an organic medium, surface modification was essential. The first approach was to use silane-type coupling agents. This method involved the use of either long-chain silane coupling agents or short-chain amino-silane type agents being extended by reaction with acid chlorides. However, the use of silane coupling agents did not yield the desired results. For instance, the long-chain silane coupling agent octadecyltrimethoxy silane had poor solubility in water, which caused the Boehmite dispersion to turn cloudy upon its addition. As an alternative, octadecyldimethyl (3-trimethoxysilyl-propyl) ammonium chloride was used. Due to its ionic part, this reagent was soluble in water and could be easily mixed with the Boehmite dispersion. Following the treatment, it was attempted to transfer the Boehmite particles into toluene, but they flocculated instantly. As the short-chain amino-silanes, γ-aminopropyl triethoxysilane and *N*-β-(aminoethyl)-γ-aminopropyl triethoxysilane were used. These reagents were soluble in water and they could be mixed with the Boehmite dispersion without any problem. However, further attempts to make them react with acid chlorides did not yield the intended results. The addition of acid chlorides caused the flocculation of Boehmite particles. Further attempts to freeze–dry Boehmite particles out of the cloudy suspensions in order to disperse them in different solvents were also not successful.

Another method was the use of an ionic surfactant; in our case it was dodecylbenzenesulfonic acid. This was a convenient method, since the surfactant could be added directly into the aqueous Boehmite dispersion, followed by the slow addition of organic solvent and distillation. Boehmite dispersions in toluene that were prepared accordingly, seemed to be homogeneous and birefringent. The method had the advantage that any polymer soluble in toluene could be blended with the Boehmites (in toluene) and nanocomposites could be prepared by solution casting. However, detailed TEM analysis on the composites (polystyrene–Boehmite) indicated the presence of Boehmite aggregates in the polymer. As the next attempt, we tried the grafting of Boehmite surface with short chains of modified polyisobutene (SAP230, Shell Lab) [6]. As this method contained several distillation steps, it turned out to be not very practical, especially for preparing large quantities of dispersions.

After these trials, a different approach was taken, which was to leave the Boehmite particles in their original aqueous environment and to use a water-soluble monomer that could be in situ polymerised to yield the polymer–Boehmite nanocomposites. For this purpose, ε-caprolactam was selected as the water-soluble monomer. Polyamide-6–Boehmite nanocomposites could be prepared successfully by this method. The preparation method and properties of the nanocomposites have been described in detail in our previous publication [11].

1.3. Present work

In this work, we have followed the same in situ polymerisation method as described above, but with some modifications. This time, a titanate type coupling agent (KR–44, Kenrich Chemicals) has been applied on Boehmites (Fig. 1). The particles are then more stable and they can be transferred into ε-caprolactam with complete evaporation of the solvent. By this modification of the former method, the problems encountered with high water contents during the polymerisation can be avoided and thus, it becomes easier to reach higher particle contents in the polymer.

2. Experimental

2.1. Boehmite synthesis

Synthesis and characterization of Boehmite needles were performed in collaboration with the group of Lekkerkerker (Colloid Chemistry Group, Utrecht University), using the well-defined method of Buining et al. [12]. The procedure has been described in more detail in our previous publication [11]. The synthesis yielded Boehmite needles in stable aqueous dispersions, at a pH of 5.5. Starting from a concentration of 0.8% (w/w), the dispersions were flow birefringent and they turned to be permanently birefringent above 1% (w/w). Boehmite concentration in aqueous dispersions used in the polymerisation reactions was 0.93% (w/w). As for the dimensions of Boehmite needles, TEM characterization revealed an average length of 280 nm and an average width of 20 nm.

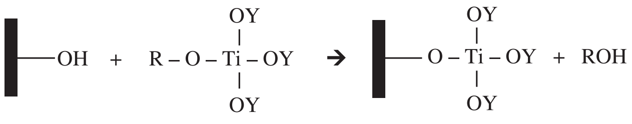

$$\text{—OH} + \text{R–O–}\overset{\text{OY}}{\underset{\text{OY}}{\text{Ti}}}\text{–OY} \rightarrow \text{—O–}\overset{\text{OY}}{\underset{\text{OY}}{\text{Ti}}}\text{–OY} + \text{ROH}$$

Fig. 1. Schematic representation of a monoalkoxy type titanate agent coupling to an inorganic surface with hydroxyl groups.

2.2. Surface modification of Boehmite

As mentioned before, we used a titanate-type coupling agent for the surface modification of Boehmite: titanium IV, tris[2-[(2-aminoethyl)amino]ethanolato-O],2-propanolato (obtained from Kenrich Chemicals with the commercial name KR-44) [10]. First, *n*-propanol (Acros organics) was added drop wise into the Boehmite (aq) dispersion under ultrasonication. This was followed by azeotropic distillation with further addition of *n*-propanol to maintain a constant volume. In the end, a stable dispersion of Boehmite in propanol was obtained. The change of solvent was required as the first step, because of insolubility of the Ti-coupling agent in water. Finally, the coupling agent in propanol was introduced in a drop wise manner into the dispersion, accompanied by ultrasonication.

2.3. Preparation of PA6 nanocomposites

In our previous work, polyamide-6 was obtained from ε-caprolactam by using the hydrolytic ring opening polymerisation method. Because of its success in obtaining PA6-nanocomposites, the same method has been used for this work [13]. As for the melt polymerisation set-up, a 500 ml glass reactor coupled with an automatic stirrer and a temperature controller was used. The monomer, ε-caprolactam (Fluka) was used without purification. Proportions of reactants were the following: 40 g ε-caprolactam, 0.25 g adipic acid (Fluka), 10 g aminocaproic acid (Aldrich) and 5–10 ml of demineralized water (as the initiator). The reaction mixture was first heated at 150 °C for 2 h to remove excess water and then it was kept at 230 °C for 4 h to facilitate the polymerization. Following this treatment, the polymeric products were subjected to Soxhlet extraction in methanol during 12 h, for purification from unreacted monomer and oligomers.

In the presence of titanate-modified Boehmite needles, the procedure was slightly modified. The dispersion of particles in *n*-propanol was combined with ε-caprolactam to form a homogeneous mixture. Propanol was expelled completely in the rotavap leaving a solidified mixture of monomer containing the titanate-modified Boehmite

Table 1
Titanate-modified Boehmite contents of the nanocomposite samples as determined from TGA measurements

Sample name	Boehmite content (wt%)
PA6-Ti-BOE1	1.1
PA6-Ti-BOE3	3.2
PA6-Ti-BOE5.5	5.5
PA6-Ti-BOE7	7.1
PA6-Ti-BOE13	12.7
PA6-Ti-BOE15	14.9

particles, which was then introduced to the melt polymerisation set-up. As a result of this treatment, PA6 nanocomposites containing about 1; 3; 5.5; 7; 13 and 15 wt% titanate-modified Boehmite were obtained, see Table 1.

2.4. Sample preparation

For further characterization, polymer samples were pressed into thin films by using a hydraulic press. The temperature of the press was 250 °C and the applied force was approximately 180 kN. The final film thickness was about 0.3 mm. Sample films were extensively dried and stored in a vacuum oven at 80 °C.

2.5. Transmission electron microscopy (TEM)

Transmission electron microscopy (TEM) was performed using a Philips CM30T electron microscope with a LaB6 filament operated at 300 kV. Ultramicrotomed samples were placed on quantifoil carbon polymer supported on a copper grid.

2.6. Atomic absorption spectroscopy (AAS)

Titanium content of the sample solutions was analysed with the ICP-OES technique by using a Perkin–Elmer Plasma 40 atomic absorption spectrometer. All solutions were diluted with water to reach the concentration range where the instrument was calibrated and acidified with nitric acid to 0.5 M. The blank Boehmite solution did not contain a detectable amount of titanium.

2.7. Differential scanning calorimetry (DSC)

The measurements were performed on a Perkin–Elmer DSC7 differential scanning calorimeter. Samples were heated from 25 to 250 °C at a rate of 10 °C/min and were held at 250 °C for 1 min. They were cooled back to 25 °C at a rate of 10 °C/min, which was followed by a second heating run identical to the first.

2.8. Dynamic mechanical analysis (DMA)

Storage modulus values were measured in the extension mode at 1 Hz frequency, using a Perkin–Elmer DMA 7e dynamical mechanical analyser. The measurements were taken in the interval 25–160 °C at a heating/cooling rate of 5 °C/min. A small rectangle of 9–7 mm long and 2.5 mm wide was cut from each pressed sample. As mentioned above, the sample thickness was 0.3 mm after the pressing.

2.9. Thermogravimetric analysis (TGA)

The exact titanate-modified Boehmite content of the nanocomposite samples was determined by using TGA. The samples were heated from 25 to 800 °C at a rate of 50 °C/min and were kept at this temperature for 30 min. As the polymer degraded completely at this temperature, the residual weight was due to the inorganic content. Weight loss of freeze-dried titanate-modified Boehmite particles as measured in TGA was taken as reference.

3. Results and discussion

3.1. Characterization of the surface modification

Titanate-modified Boehmite dispersions in *n*-propanol were transparent and quite stable over time. Dispersions were kept for a few months after preparation and no sign of phase separation was observed. The stability of Boehmite needles in *n*-propanol before and after the surface treatment is clearly illustrated by the TEM pictures (Fig. 2(a) and (b)).

In order to get a quantitative measure of the titanate agent present on the Boehmite surface, atomic absorption spectroscopy (AAS) was performed. For this purpose, identical amounts of Boehmite dispersions were treated with varying amounts of the titanate agent. After equilibration, the

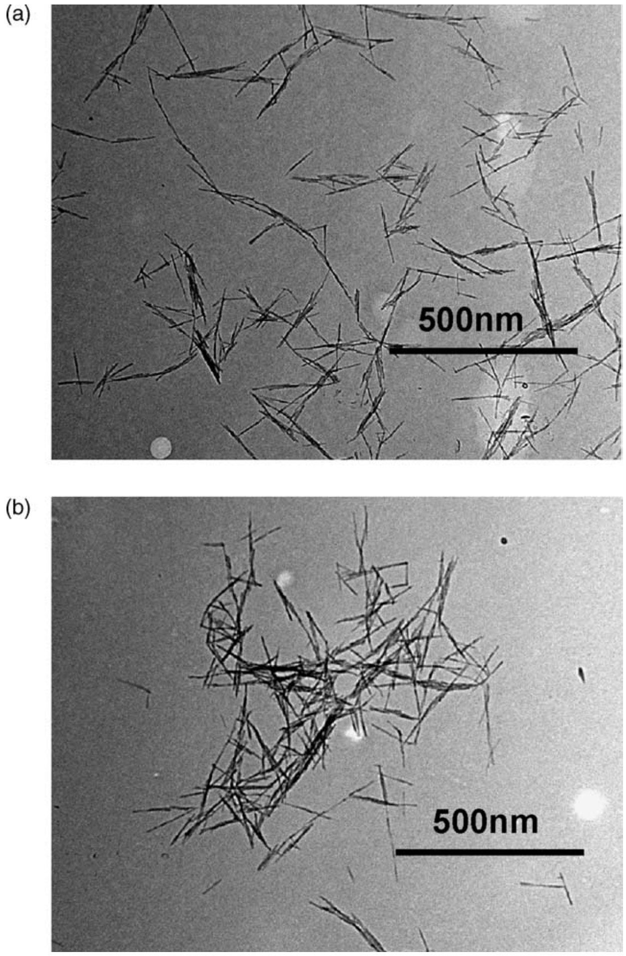

Fig. 2. (a) TEM picture of the Boehmite needles stabilised in *n*-propanol. (b) TEM picture of the Boehmite needles in *n*-propanol after treatment with the titanate agent.

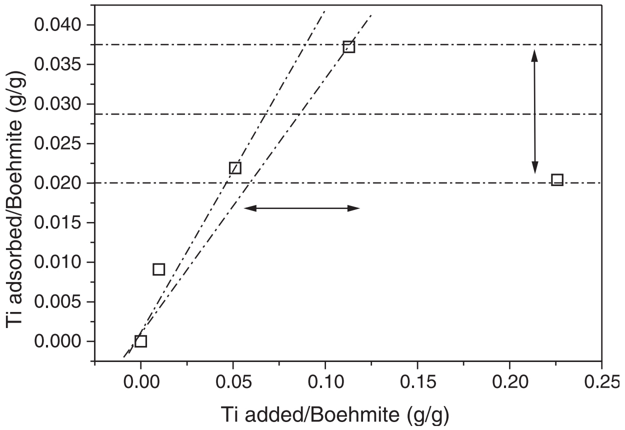

Fig. 3. The amount of grams of titanate agent adsorbed/g Boehmite with respect to the introduced amount of agent.

Boehmite needles could be precipitated by centrifugation. Supernatant parts were analysed for their Ti-content using AAS. By this method, the amount of titanate agent retained on the Boehmite surface could be calculated [14]. Fig. 3 shows the amount of grams of titanate agent adsorbed per gram of Boehmite with respect to the introduced amount of titanate agent.

As expected, grams of adsorbed Ti-agent/g Boehmite values show a linear increase with added amount of the titanate agent. However, following the linear increase regime, it is difficult to assign a general behaviour based on the single data point. It is not clear whether the decrease in that data point is a fluctuation or an indication that after a certain level, grams of adsorbed Ti-agent/g Boehmite values do not increase any further. By looking at the overall trend, it can be speculated that the amount of adsorbed Ti-agent does not increase further beyond the point of 0.038 g/g Boehmite. If we make the assumption that the values remain constant after this point, we can claim that the maximum amount of adsorbed Ti-agent is in the range of 0.020–0.035 g/g Boehmite. However, this is only a crude estimation and should not be considered very accurate.

3.2. Distribution of titanate-modified Boehmite in PA6 nanocomposites

TEM analysis has been performed on the PA6-Ti-BOE7 and PA6-Ti-BOE15 samples. For both samples, titanate-modified Boehmite particles are distributed homogeneously throughout the polymer (Figs. 4(a) and 5). It is also clear from these pictures that more rods are present for PA6-Ti-BOE15 than for PA6-Ti-BOE7. In certain regions of the PA6-Ti-BOE15 sample, very distinct nematic orientation of the rods is observed. As for PA6-Ti-BOE7, two different images are shown: Fig. 4(a) shows the image obtained in the plane containing the rods. Fig. 4(b) shows the image in the perpendicular plane, and thus gives a cross-sectional view of the rods. The cross sectional image shows a homogeneous alignment pattern, which indicates that this sample also exhibits some nematic orientation.

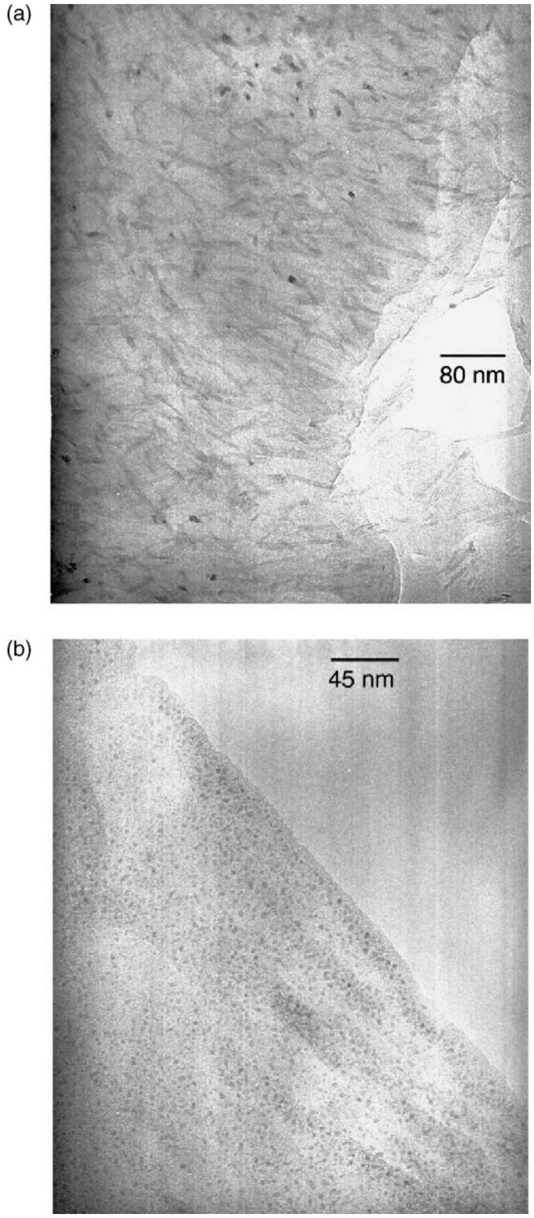

Fig. 4. (a) TEM picture of the PA6-Ti-BOE7 sample (in-plane with the rods). (b) TEM picture of the PA6-Ti-BOE7 sample (perpendicular to the plane with the rods).

3.3. Thermal properties

A detailed thermal analysis of the samples has been carried out by using DSC. Samples were subjected to heating from 25 to 250 °C at a rate of 10 °C/min, which was followed by cooling back to 25 °C at the same rate. After this, a second heating run was performed with the identical parameters.

As in our previous work, we preferred to focus on the second heating cycle rather than the first. The reason was to

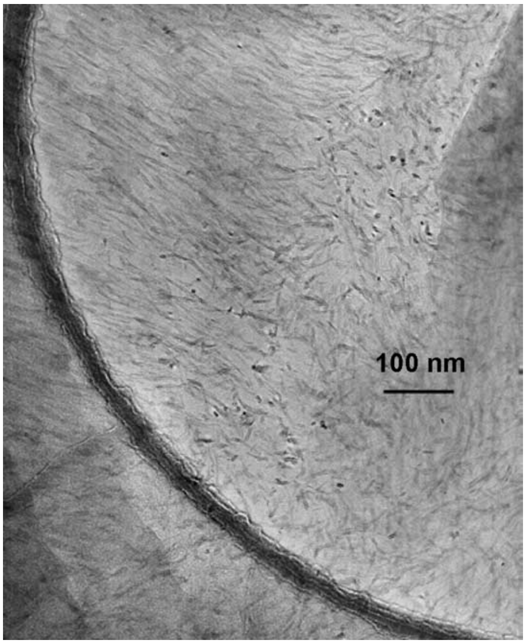

Fig. 5. TEM picture of the PA6-Ti-BOE15 sample.

investigate the real crystallization effects without being dependent on the differences in preparation and thermal history of the samples. For a quantitative analysis of the second heating, curve fitting was performed. Using the Excel program, Gaussian functions were used to fit the DSC peaks and peak integrals were calculated. For the first heating, analysis of peaks was done only qualitatively. Because the crystallization peaks are very similar, the curves are not shown here, but only the crystallization temperatures are given.

In Fig. 6, the melting curves of PA6-Ti-BOE1, 3, 5.5, 7, 13 and 15 samples obtained during the first heating are shown. The figure indicates that the intensity of the first peak, which appears around 210 °C, increases with the titanate-modified Boehmite content. It appears initially as a small shoulder, and then is resolved into a well-defined peak at 210 °C. This peak is known as the melting peak of the γ-phase of polyamide-6. The second melting peak, which is due to the melting of the α-phase, appears around 220 °C for all samples [15–20].

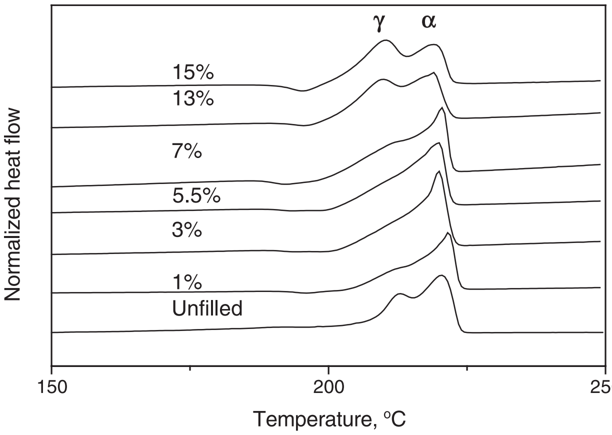

Fig. 6. DSC melting curves of PA6-unfilled and PA6-Ti-BOE1, 3, 5.5, 7, 13 and 15 (from bottom to top) obtained in the first heating cycle.

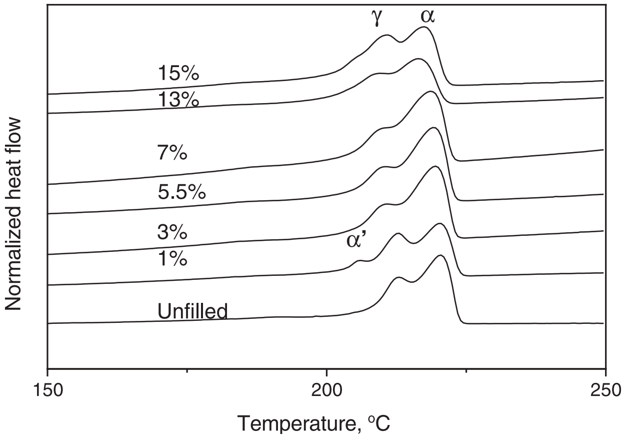

Fig. 7. DSC melting curves of PA6-unfilled and PA6-Ti-BOE1, 3, 5.5, 7, 13 and 15 (from bottom to top) obtained in the second heating cycle.

As the second heating cycle is concerned, one can observe very clearly the melting peaks of γ- and α-phases. Fig. 7 shows the melting curves of PA6-Ti-BOE1, 3, 5.5, 7, 13 and 15 samples obtained in the second heating cycle. The γ-peak is present from the beginning of the concentration series, which is different from the first cycle. The only change is in the relative intensities of the two peaks with titanate-modified Boehmite concentration. Here, it is essential to look at the peak integrals in order to make some quantitative discussions over the intensities. In Table 2, melting temperatures and enthalpies of γ- and α-phases present during the second heating cycle are given. The enthalpy values are calculated by taking the integrals of the fitted Gaussian curves.

Going from PA6-Ti-BOE1 to higher concentrations, there is a general tendency in $T_{\mathrm{melt}}\gamma$, $T_{\mathrm{melt}}\alpha$ and T_{cryst} values to decrease slightly. In addition, $\Delta H_{\mathrm{melt}}\gamma$ values increase noticeably for PA6-Ti-BOE13 and PA6-Ti-BOE15. The

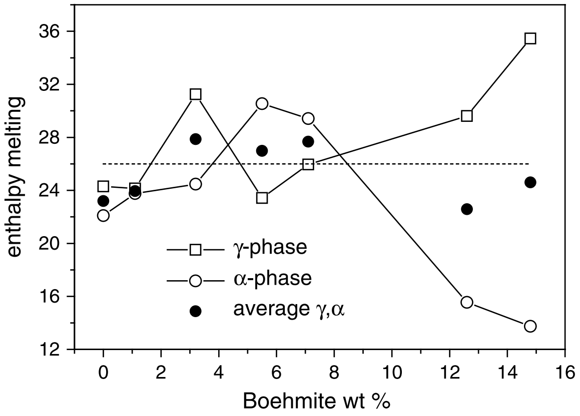

Fig. 8. Enthalpy of melting for the α- and γ-phases observed in the second heating cycle as a function of Boehmite concentration.

Table 2
Melting temperatures and enthalpies of the α- and γ-phases in the second heating cycle and crystallization temperatures

Sample	$T_{\mathrm{melt}}\gamma$ (°C)	$\Delta H_{\mathrm{melt}}\gamma$ (J/g)	$T_{\mathrm{melt}}\alpha$ (°C)	$\Delta H_{\mathrm{melt}}\alpha$ (J/g)	T_{cryst} (°C)
PA6-Ti-BOE1	212.8	24.14	220	23.76	184
PA6-Ti-BOE3	212.5	31.25	219.3	24.47	183.8
PA6-Ti-BOE5.5	211	23.42	218.9	30.54	182.3
PA6-Ti-BOE7	211	25.95	218.4	29.42	183.6
PA6-Ti-BOE13	210	29.61	216.9	15.55	179
PA6-Ti-BOE15	210.6	35.46	217.8	13.75	180.3

values for $\Delta H_{\mathrm{melt}}\alpha$ are close to those of $\Delta H_{\mathrm{melt}}\gamma$ for low Ti-BOE contents. They slightly increase for PA6-Ti-BOE5.5 and 7 and then undergo a substantial decrease for PA6-Ti-BOE13 and 15 (15–14 J/g). Although the sum of $\Delta H_{\mathrm{melt}}\alpha$ and $\Delta H_{\mathrm{melt}}\gamma$ values is not completely constant, it is still possible to conclude that the relative amounts of these phases are dependent on each other. To get a better view of this, $\Delta H_{\mathrm{melt}}\alpha$ and $\Delta H_{\mathrm{melt}}\gamma$ values from Table 2 are plotted as a function of Boehmite concentration in Fig. 8.

The total enthalpies of melting and crystallization are given in Table 3. $\Delta H_{\mathrm{melt}}1$ and $\Delta H_{\mathrm{melt}}2$ refer to the first and the second heating cycles. % Crystallinity values have been calculated using the following equation [18]:

$$X_{\mathrm{C}}(\%) = \frac{\Delta H_{\mathrm{cryst}}}{\Delta H^{0}_{\mathrm{melt}}} \times 100 \quad (1)$$

$\Delta H_{\mathrm{cryst}}$ is the enthalpy of crystallization, which is normalised per gram of PA6. $\Delta H^{0}_{\mathrm{melt}}$ is the enthalpy of melting for a 100% crystalline polyamide-6 and is taken as an average value of 190 J/g [18,21]. Comparison of enthalpy of melting values within the concentration series does not provide any significant trend. It can be speculated that enthalpy of crystallization and % crystallinity values show a slightly decreasing trend, although not obvious from the table. In order to observe this trend more clearly, enthalpy of crystallization values from Table 3 are plotted as a function of Boehmite content in Fig. 9.

In our previous work on unmodified Boehmite–PA6 nanocomposites, we observed the γ-phase to be the most abundant in the second heating cycle. Moreover, we reported the emergence of a new peak at higher filler concentrations (Fig. 10). While the amount of the γ-phase was almost constant, competition occurred between the α- and α′-phases.

In contrast, the α′-phase is not observed in the PA6-titanate-modified Boehmite series. It only appears in the first sample, PA6-Ti-BOE1 with low intensity. Instead, the interplay occurs between the γ- and α-phases, as the amount of the γ-phase increases and that of the α-phase decreases with Boehmite content.

Another difference is related to the melting temperatures. Going from PA6-Ti-BOE1to higher concentrations, there is a general tendency in $T_{\mathrm{melt}}\gamma$ and $T_{\mathrm{melt}}\alpha$ values to decrease slightly, which is an effect that was not observed with unmodified Boehmites. The presence of the surface modification apparently has a slight effect on the melting temperatures.

The conclusion to be drawn from this comparison is that the surface modification clearly affects the interaction of the Boehmite particles with the PA6 chains. Titanate modified Boehmite particles favour the formation of the γ-phase, as is the case for many other inorganic filler-PA6 nanocomposites. The amino-end groups of the titanate agent should be capable of forming hydrogen bonds with the PA6 chains. However, compared to unmodified Boehmite, the hydrogen bonding units are less ordered due to these factors: (1) the exact location of the titanate molecules on Boehmite is not well-defined, (2) the amino-end groups are more randomly oriented in space, compared to the more ordered surface hydroxyls of the Boehmite. These factors result in a ‘soft’ interaction of titanate-modified Boehmites with the PA6 chains, which does not provide a constraint for the crystallization and as a result, the α′-phase of PA6 present in the case of unmodified Boehmites, is not observable here.

In the above analysis using DSC, the conclusions are mainly based on the comparison of the results for polyamide-6 nanocomposites with unmodified and titanate-modified Boehmite. For both series of nanocomposites,

Table 3
Total enthalpies of melting (cycle 1 and 2) and crystallization and calculated % crystallinity of the samples

Sample	$\Delta H_{\mathrm{melt}}1$ (J/g)	$\Delta H_{\mathrm{melt}}2$ (J/g)	$\Delta H_{\mathrm{cryst}}$ (J/g)	% Crystallinity
PA6-unfilled[a]	60.86	65.71	−77.66	40.9
PA6-Ti-BOE1	61.12	68.07	−62.54	32.9
PA6-Ti-BOE3	68.51	71.71	−68.23	35.9
PA6-Ti-BOE5.5	65.69	69.54	−64.75	34.1
PA6-Ti-BOE7	66.49	69.82	−67.98	35.8
PA6-Ti-BOE13	52.75	58.67	−54.28	28.6
PA6-Ti-BOE15	57.94	67.48	−59.06	31.1

[a] The values for PA6-unfilled are taken from our previous work.

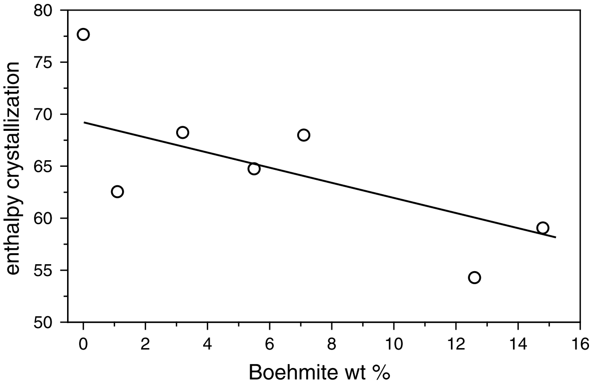

Fig. 9. Enthalpy of crystallization as a function of Boehmite concentration.

the DSC results are obtained by using identical experimental procedures. It should be realized that the DSC technique might give difficult to interpret results for the melting behaviour due to possible recrystallization of the polymer. In addition to DSC, further characterization of the samples by using X-ray diffraction is in progress, and these results seem to be in agreement with the DSC results. This part of the characterization will be the topic of a future publication, which also reports results on the level of orientation of Boehmite particles.

3.4. Mechanical properties

As stated in Section 2, storage moduli of the samples have been measured during heating and cooling in the temperature interval of 25–160 °C. The modulus values obtained in the cooling part of the curve were higher compared to the heating part. Since the samples were possibly still drying during the heating cycle, the cooling part was taken to be more reliable. In order to make sure that the modulus values reached constant values in the end, an isothermal run at 25 °C was performed for each sample, following the cooling part.

In Fig. 11, storage modulus values measured in the interval 160 °C to room temperature are given. The samples follow a very systematic trend. The first two samples, namely PA6-Ti-BOE1 and PA6-Ti-BOE3 do not exhibit any significant difference in the range. However, starting from PA6-Ti-BOE5.5, storage moduli increase systematically and the increase is valid for all temperatures in this interval. The curves reach their maximum values at the end of the cooling cycle, namely at 36 °C. As mentioned above, each sample was subjected to an isothermal measurement following the temperature cycle. As a result of the dynamical mechanical analysis, it is observed that the storage modulus values of the PA6-Ti-BOE nanocomposites can go up to 4.23 GPa at the maximum Boehmite concentration. This is 1.8 times the modulus of the sample with the lowest Boehmite concentration (PA6-Ti-BOE1). With respect to the unfilled PA6, this is a two-fold improvement.

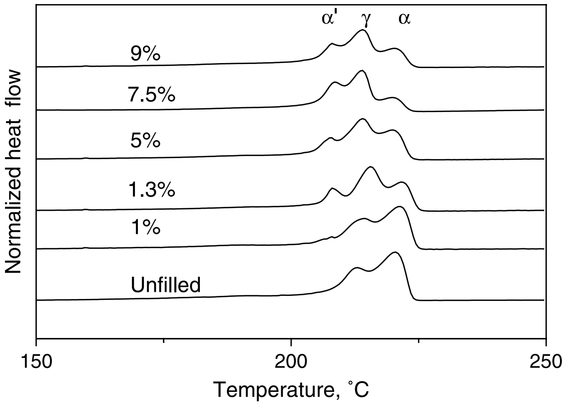

Fig. 10. DSC second heating curves of PA6-unfilled and PA6-BOE1, 1.3, 5, 7.5 and 9 (from bottom to top), which are the PA6 samples containing unmodified Boehmite as described in our previous work.

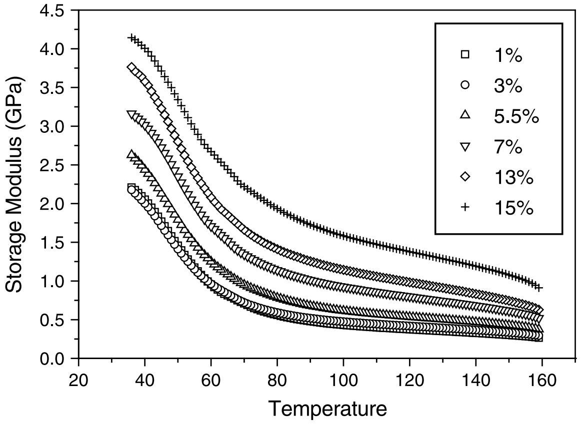

Fig. 11. Storage modulus E' curves of the samples in the temperature interval 37–160 °C measured at 1 Hz frequency.

3.5. Comparison with mechanical models

The results obtained with the PA6-Ti-BOE system have been compared to some mechanical composite models, including the model for randomly oriented fibers (in two- and three-dimensions) and the Halpin–Tsai model. So far, the Halpin–Tsai model gives the best explanation for the data.

The equations in the Halpin–Tsai model are as follows:

$$\frac{M_\mathrm{c}}{M_\mathrm{m}} = \frac{1+\zeta\eta c_\mathrm{r}}{1-\eta c_\mathrm{r}} \tag{2}$$

with

$$\eta = \frac{\left(\dfrac{M_\mathrm{r}}{M_\mathrm{m}} - 1\right)}{\left(\dfrac{M_\mathrm{r}}{M_\mathrm{m}} + \zeta\right)} \tag{3}$$

In this notation, M_r, M_m and M_c are the modulus of the filler, of the matrix and of the composite, respectively. c_r

denotes the volume fraction of the filler and ζ is a factor that depends on the geometry of the filler particle and the type of modulus to be calculated. The elastic constants in different directions in the matrix can be obtained by using this model. In the case of unidirectional short fiber composites, the modulus improvement is expected to occur in the longitudinal direction along the short fibers, so it is sufficient to calculate one elastic constant.

The modulus in the longitudinal direction is related to the elastic constant denoted by E_{33}. In this case, $\zeta = 2l/d$ is used for the geometric factor (l: fiber length, d: fiber thickness). The equations mentioned above have been used to calculate the storage modulus values of the PA6-Ti-BOE nanocomposites. In these calculations, the modulus of the matrix is taken as 2.03 GPa, which is the experimental value for the unfilled PA6. The Young's modulus for the filler is taken as 253 GPa [22]. In order to convert the concentrations from weight percentages to volume fractions, $d_{\mathrm{PA6}} = 1.13\ \mathrm{g/cm^3}$ and $d_{\mathrm{Boehmite}} = 3.01\ \mathrm{g/cm^3}$ [3] have been used.

The results obtained with the Halpin–Tsai model are shown together with the experimental results of the PA6-Ti-BOE and the previous PA6-BOE series [11] in Fig. 12.

To summarize the mechanical properties of the system, we have observed a two-fold increase in storage moduli with respect to the pure matrix. The experimental curve can be fitted nicely by the Halpin–Tsai model. Although the curve shows a similar trend compared to the PA6-unmodified Boehmite series, this new method allows us to obtain higher Boehmite contents in the matrix; and as a consequence, higher modulus values.

4. Conclusions

A modification method has been described for Boehmite, which involves the use of a titanate coupling agent. By modification, Boehmite particles are stabilized in the monomer itself, which can be directly polymerised. This method eliminates the necessity to introduce the particles as dispersions in water. The used propanol can in principle be removed completely before starting the polymerisation. As a result of this treatment, the problems encountered in the PA6 polymerisation due to high water contents can be avoided and with respect to the nanocomposites with unmodified Boehmites, higher particle loadings can be achieved.

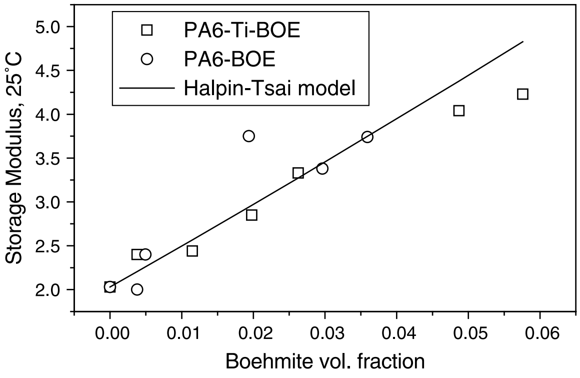

Fig. 12. A comparison of the storage modulus values of PA6-Ti-BOE with the previous PA6-BOE samples and with the Halpin–Tsai model.

TEM analysis proves homogeneous dispersion of particles in the polymer matrix. Cross-sectional and in-plane images of the PA6-Ti-BOE7 sample indicate alignment of the rod-like particles at this concentration. The PA6-Ti-BOE15 sample has higher extent of nematic alignment reflected by the presence of more aligned areas in the TEM image. In a future publication, the alignment phenomenon will be investigated in more detail.

The nanocomposites show gradual improvement in mechanical properties with increasing amount of titanate-modified Boehmite. The maximum value of Young's modulus is observed as 4.23 GPa at 15% particle content, which is almost twice the value of unfilled PA6. Comparison of data points of nanocomposites containing titanate-modified with those containing unmodified Boehmite shows that they follow a similar behaviour that can be fitted nicely with the Halpin–Tsai model.

Titanate-modified Boehmites also favour the crystallization of PA6 in the γ-form rather than the α-form at high particle contents. Thermal properties of PA6-Ti-BOE samples differ slightly from the PA6-BOE's, as the α'-phase of PA6 is not observed in the former. It is likely that the surface modification alters the interaction of Boehmite particles with the polymer chains. Although the hydrogen bonding still exists, the random orientation and position of hydrogen bondable surface groups has less constraint on the α-crystallization.

Acknowledgements

We acknowledge Prof H.N.W. Lekkerkerker and D. van der Beek of Colloid Chemistry Group, Utrecht University for their help in the Boehmite synthesis. Dr Adam Best is highly appreciated for his valuable comments and discussions. S.J. Monte from Kenrich Petrochemicals, Inc. is deeply acknowledged for supplying the coupling agent, KR-44 and very useful information. We thank Dr P.J. Kooyman of the National Center for High Resolution Electron Microscopy, TU Delft for performing the TEM analysis. Ben Norder of the Polymer and Materials Engineering, TU Delft is acknowledged for the DMA and DSC measurements. Joop Padmos of the Delft Chem Tech, TU Delft is acknowledged for the AAS measurements. This work forms as part of the research program of the Dutch Polymer Institute.

References

[1] Okada K, Nagashima T, Kameshima Y, Yasumori A, Tsukada T. J Colloid Interf Sci 2002;253:308.

[2] Musić S, Dragcević D, Popović S, Vdović N. Mater Sci Eng B 1998;52:145.

[3] Buining PA. Preparation and properties of dispersions of colloidal Boehmite rods. Utrecht: PhD Thesis; 1992.

[4] Philipse AP, Nechifor AM, Pathmamanoharan C. Langmuir 1994;10:4451.

[5] Van Bruggen MPB. Langmuir 1998;14:2245.

[6] Buining PA, Veldhuizen YSJ, Pathmamanoharan C, Lekkerkerker HNW. Colloid Surf 1992;64:47.

[7] Levering AW. Interphases in zirconium silicate filled high density polyethylene and polypropylene. Delft: PhD Thesis; 1995.

[8] Plueddemann EP. Silane coupling agents. New York: Plenum Press; 1982.

[9] Mitsuishi K, Yabuki T, Kodama S, Kawasaki H. J Mater Sci Lett 1989;8:624.

[10] Monte SJ. Polym Polym Compos 2002;10:1.

[11] Ozdilek C, Kazimierczak K, Van der Beek D, Picken SJ. Polymer 2004;45:5207.

[12] Buining PA, Pathmamanoharan C, Jansen JBH, Lekkerkerker HNW. J Am Ceram Soc 1991;74:1303.

[13] Pielichowski J, Puszynski A. Polymer preparation methods. Krakow: Technical University of Krakow; 1978.

[14] Van Bruggen MPB, Donker M, Lekkerkerker HNW, Hughes TL. Colloid Surf A 1999;150:115.

[15] Kojima Y, Usuki A, Kawasumi M, Okada A, Fukushima Y, Kurauchi T, et al. J Mater Res 1993;8(5):1185.

[16] Liu L, Qi Z, Zhu X. J Appl Polym Sci 1999;71(7):1133.

[17] Wu T, Liao C. Macromol Chem Phys 2000;201:2820.

[18] Liu X, Wu Q, Berglund LA, Qi Z. Macromol Mater Eng 2002;287:515.

[19] Fornes TD, Paul DR. Polymer 2003;44:3945.

[20] Yasue K, Katahira S, Yoshikawa M, Fujimoto K. In: Pinnavaia TJ, Beall G, editors. Polymer–clay nanocomposites. New York: Wiley; 2000.

[21] Aharoni SM. *n*-Nylons: their synthesis, structure and properties. Wiley: WestSussex; 1997.

[22] Gallas MR, Piermarini GJ. J Am Ceram Soc 1994;77:2917.